# Ecological impact of mechanical cleaning method to curb black stain alterations on Paleolithic cave walls

Zélia Bontemps, Mylène Hugoni, Yvan Moënne-Loccoz

International Biodeterioration & Biodegradation 191 (2024) 105797

Contents lists available at ScienceDirect

International Biodeterioration & Biodegradation

journal homepage: www.elsevier.com/locate/ibiod

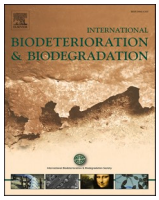

# Ecological impact of mechanical cleaning method to curb black stain alterations on Paleolithic cave walls

Zélia Bontemps [a], Mylène Hugoni [a,b,c], Yvan Moënne-Loccoz [a,*]

[a] Univ Lyon, Université Claude Bernard Lyon 1, CNRS, INRAE, VetAgro Sup, UMR 5557 Ecologie Microbienne, F-69622, Villeurbanne, France
[b] Univ Lyon, Université Claude Bernard Lyon 1, CNRS, INSA de Lyon, UMR 5240 Microbiologie Adaptation et Pathogénie, F-69622, Villeurbanne, France
[c] Institut Universitaire de France (IUF), Paris, France

ARTICLE INFO

*Keywords:*
Paleolithic caves
Microbial alterations
Microbial contamination
Cave conservation strategy
Recolonization indicators
Ecological impact

ABSTRACT

Anthropization of Paleolithic karstic caves can cause an imbalance of cave microbiota and may trigger formation of wall alterations including black stains. In Lascaux Cave, a previous attempt to mechanically remove black stains was followed by reformation of the stain in months, suggesting that microbial recolonization had taken place. On this basis, we hypothesized that mechanical cleaning (a routine cleaning method for conservation of heritage sites) leaves a residual microbial community that can also serve as pioneer community, i.e. a community of early microbial residents that triggers subsequent microbial successions involved in the reformation of black stains. We monitored post-cleaning microbial recolonization over 19 months in the Apse of Lascaux Cave (France), after using two methods of mechanical cleaning (scalpel alone, or scalpel + sponge). Illumina MiSeq metabarcoding evidenced various taxa i.e. the bacteria *Pseudomonas*, *Pedomicrobium* and black-melanized fungi *Ochroconis* (=*Scolecobasidium*) during early recolonization of cleaned surfaces, and at later stages the establishment of several other taxa including the bacteria *Luteimonas, Chitinophaga* and the black fungus *Exophiala*. Surfaces at 19 months after cleaning were visually and microbiologically different from stained surfaces immediately after cleaned and from unstained surfaces, but also from non-cleaned stained surfaces, probably because of a particular microbial succession, distinct from the original succession during stain formation. Variations in relative abundance of Bacteroidota and Eurotiomycetes classes and *Exophiala* genus were higher when the sponge was used in addition to the scalpel. The bacteria *Filomicrobium* and the fungi *Isaria* and *Cephalotrichum* were identified on sponge-cleaned surfaces and on the sponge itself, pointing to a contaminant status due to the cleaning method. Overall, it suggests that post-cleaning pioneer communities may play an important role in orienting stain reformation in caves. Sponges routinely used by restorers to curb microbial stains may bring microbial contaminants, which questions current cleaning practices in show caves.

## 1. Introduction

Limestone regions display karstic underground ecosystems, and many caves have been used by prehistoric humans for shelter or parietal art, leading to contemporary touristic activities in many of them. Tourism is also significant in a broad range of caves with outstanding geological features, such as speleothems or underground water bodies (Cigna, 2016).

Show caves have undergone substantial environmental changes, first as a consequence of transformations implemented for visits, i.e. installation of a light systems, etc. (Cigna, 2016). Second, the visitors consume oxygen, release $CO_2$ and may deposit organic matter (Jurado et al., 2010). These effects may cause an imbalance in the cave microbiota (Pfendler et al., 2018). It might lead to abnormal microbial growth and the formation of surface alterations on cave walls. Consequently, several show caves were closed to the public, in particular the iconic UNESCO caves Altamira (Spain) and Lascaux (France) (Barton and Jurado, 2007; Bastian et al., 2010; Cigna, 2016).

Different surface alterations have been reported on cave walls, with stains corresponding to microbial constituents e.g. melanin (black) from fungal cell walls (De la Rosa et al., 2017) or carotenoids (brown/orange) from various microorganisms (Sakr et al., 2020), or to microbial transformations, e.g. manganese precipitation by many bacterial and fungal species (Alabouvette and Saiz-Jiménez, 2011) and calcite deposition by

* Corresponding author.
*E-mail address:* yvan.moenne-loccoz@univ-lyon1.fr (Y. Moënne-Loccoz).

https://doi.org/10.1016/j.ibiod.2024.105797
Received 3 February 2024; Received in revised form 23 March 2024; Accepted 16 April 2024
Available online 30 April 2024

bacteria (Chalmin et al., 2007). Stains are commonly managed using mechanical removal and/or targeted chemical treatments, and the latter manage (or sometimes fail) to control microbial outbreaks (Bastian et al., 2009a; Diaz-Herraiz et al., 2014). In fact, the chemical treatments themselves may trigger the formation of cave wall alterations in certain cases, as illustrated with benzalkonium chloride and black stains in Lascaux Cave (Bastian et al., 2010; Martin-Sanchez et al., 2015), perhaps the most anthropized of all show caves. In Lascaux Cave, black stains represent one of the most extreme alterations, as they may develop after previous types of stains were removed by chemical treatments (Martin-Sanchez et al., 2015) and they are hard to eradicate chemically (Bastian et al., 2009b). Black stains are also documented in other caves, e.g. in Holly Saviour's cave (Zucconi et al., 2012) and Grotta del Cervo (Bernardini et al., 2021) in Italy, Driny Cave in Slovakia (Ogórek et al., 2016), or Cova Eirós in Spain (Steelman et al., 2017).

Microorganisms possibly involved in cave wall alterations have been evidenced, e.g. *Xanthomonodales* and *Thauera* in Altamira (Portillo et al., 2008) or *Ochroconis* (=*Scolecobasidium*) fungi in Lascaux (Alonso et al., 2023), but they are not always well documented. Furthermore, the microbial successions leading to their proliferation are essentially unknown, and relevant indicators to monitor cave wall health are lacking. In 2015, mechanical removal of a black stain was carried out in the Apse room of Lascaux, and a new black stain started to form in the following months, with the same size, shape and contour as the previous one, suggesting that removal of black stain microorganisms had been incomplete and that microbial recolonization was fast, questioning the sustainability of these stain-mitigation approaches. On this basis, we hypothesized that microbial successions involved in black stain formation implicate specific taxa from the very early stages (pioneer taxa) of recolonization on. In this context, it could well be that mechanical cleaning (incomplete in microbial terms, as some microorganisms remain) may have unexpected detrimental effects by triggering negative microbial successions, but here it was implemented to generate artificially a pioneer community and enable monitoring of subsequent microbial dynamics, which should help identify taxa implicated in microbial recolonization.

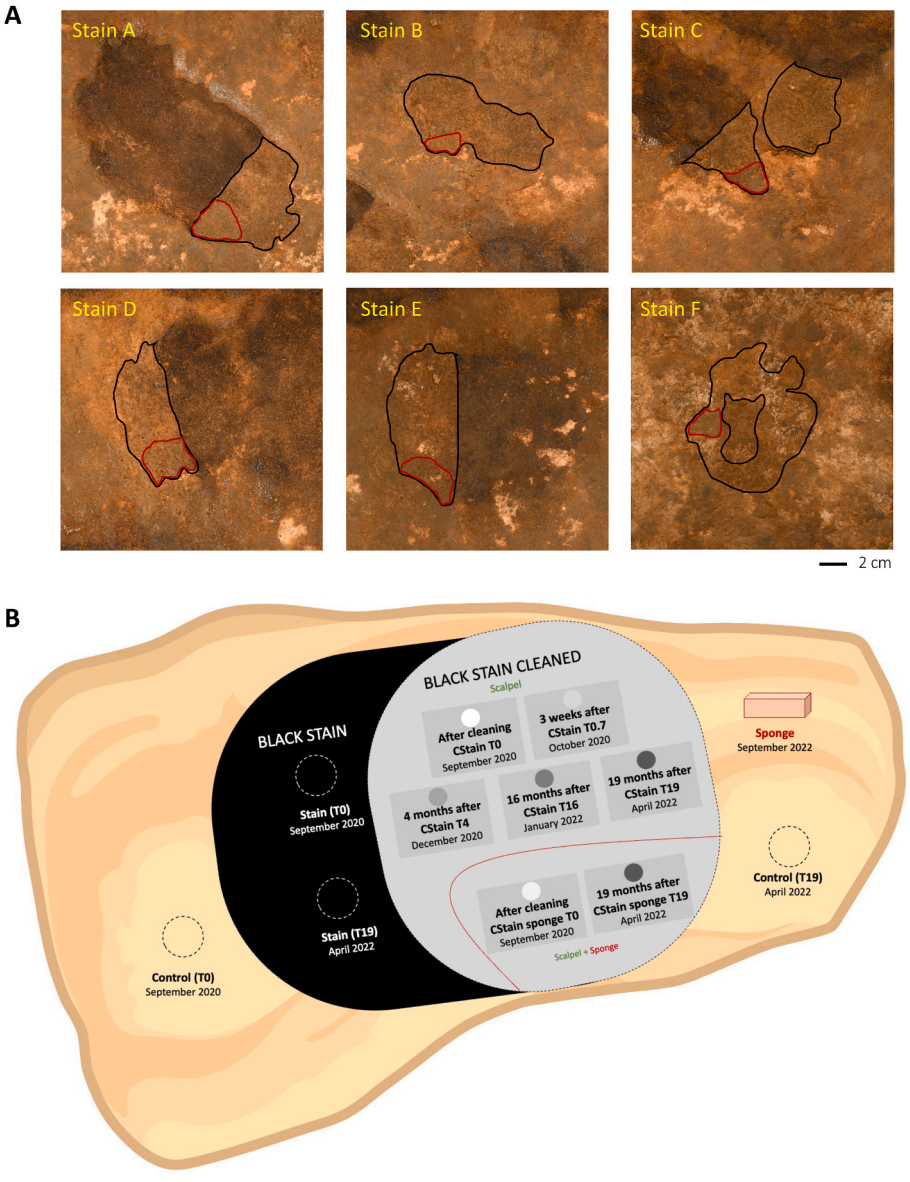


**Fig. 1.** (A) Photography of the six black stains after (partial) mechanical cleaning. The red line delimits the area cleaned with a scalpel + sponge, while the black line delimits the area cleaned only with a scalpel. The photographs show that the visual properties of cleaned areas are quite similar to those of unmarked surfaced nearby. For stain C, two neighboring areas were used. For stain F, the central part was not stained and therefore was not used. (B) Schematic layout of the samples in each rock surface condition at different sampling time, for the six replicates (A to E) of black stains cleaned. Controls conditions are represented with dotted circle.

The objective of the current work was to test this hypothesis experimentally, by characterizing the microbial successions taking place once black stains are removed by mechanical means, and identifying key microbial taxa that could serve to monitor microbial recolonization status. Six black stains in the Apse of Lascaux were manually cleaned by an accredited restorer and microbial recolonization was monitored during 19 months by MiSeq Illumina sequencing. In addition, two main mechanical cleaning methods used routinely for restoration in caves and cultural heritage sites, i.e. the use of sterile scalpel only vs sterile scalpel + sponges, were compared.

## 2. Materials & methods

### 2.1. Mechanical cleaning of black stains and sample collection

Lascaux Cave in South-West of France (N 45°03′13.087″ and E 1°10′12.362″) was closed for tourist visits in 1963 due to cave alterations. In the Apse room (30 $m^2$), which contains more than a thousand Paleolithic figures, black stains were identified on limestone wall surfaces. Here, six black stains located a small Apse area termed the Absidiole, were subjected to mechanical cleaning on September 23, 2020, using sterile disposable scalpels (Paramount #3; MDSS GmbH, Hannover, Germany) treated by gamma irradiation (Fig. 1A).

Samples from stains were collected immediately before (Stain T0 samples) and immediately after scalpel cleaning (CStain T0 - September 23, 2020), at 3 weeks (CStain T0.7–October 13, 2020), 4 months (CStain T4 - December 7, 2020), 16 months (CStain T16–January 4, 2022) and 19 months (CStain T19–April 28, 2022), using sterile scalpels, according to the authorizations given by the DRAC Nouvelle-Aquitaine (Bordeaux office, Ministry of Culture) (Fig. 1B). One sample was taken per stain and separate areas of each stain were sampled at the different dates. In addition, a control sample was taken near each black stain and on black stain on the day of mechanical cleaning and at 19 months (samples Control T0, Control T19, Stain T0 and Stain T19, respectively). Finally, one part of each black stain was cleaned with both scalpel and sponges AION D3 (AION, Japan) made of polyvinyl formal (PVFM) resin, as often done by cave restorers. Before use, the sponges had been rinsed with tap water (to remove preservatives), cut into 3 cm × 1 cm × 2 cm pieces, disinfected in boiling water for 20 min and packed in aluminum foil. Parts cleaned with scalpel and sponges AION D3 were sampled immediately after mechanical cleaning and 19 months after cleaning (samples CStain sponge T0 and CStain sponge T19) (Fig. 1B), and the surface of six unused sponges was also sampled on September 23, 2020 (samples Sponge), using scalpels. Since surfaces cleaned using a sponge were sampled immediately using scalpels (for CStain sponge T0 samples), sponges were used again after this sampling to reinstall on these areas the particular surface conditions (sponge finish) corresponding to those produced by sponge cleaning. In total, 72 samples were collected for this study. To avoid any modification of the microbial community in the samples, they were immediately placed in liquid nitrogen and transferred to −80 °C at the laboratory, until DNA extraction.

In the Apse, relative humidity is almost at saturation permanently. During the course of the study, temperature was essentially stable, as it varied between 12.9 °C and 13.2 °C (probe G1; Lharti, 2023).

### 2.2. Total DNA extraction and high-throughput sequencing

Total genomic DNA extraction was performed using the FastDNA SPIN Kit For Soil (MP Biomedicals, Illkirch, France), based on manufacturer's instructions and adjusted to small samples. Cave wall samples or sponge surface samples (about 200 mg) were placed in lysis tube, and lysis solution was added. The elution step was achieved using 90 µl of elution buffer for each sample. The DNA concentrations were quantified using the Qubit dsDNA HS Assay Kit (Invitrogen, Carlsbad, USA) following the manufacturer's instructions.

Three gene markers were analyzed in each individual sample. The V3–V4 region of the 16 S rRNA genes was amplified in triplicate for Bacteria and Archaea using the universal primers 341 F and 805 R (Herlemann et al., 2011) and 515 F and 915 R (Herfort et al., 2009), respectively (Table S1). For Eukaryota, the V4 region of the 18 S rRNA genes was amplified in triplicate using the universal primers 0067a_deg and NSR399 (Dollive et al., 2012). The PCR mix consisted in 5 µl of 5*X* Hot BioAmp Blend Master Mix RTL (Biofidal – now Microsynth, Vaulx-en-Velin, France), 0.1 µM of each primer, 0.1*X* of GC-rich-enhancer (Microsynth), 0.2 ng $\mu l^{-1}$ of bovine serum albumin (Promega, Madison, USA) and 0.2–1 ng DNA. All amplifications were performed in a Biorad T1000 thermal cycler (Biorad, Hercules, USA) using a PCR program for Bacteria composed of 3 min at 95 °C, 28 cycles of 45 s at 95 °C, 45 s at 50 °C and 90 s at 72 °C, followed by 7 min at 72 °C. For Archaea, it consisted in 10 min at 94 °C, 30 cycles of 1 min at 94 °C, 1 min at 58 °C and 90 s at 72 °C, followed by 10 min at 72 °C. For Eukarya, it consisted in 10 min at 95 °C, 30 cycles of 1 min at 94 °C, 1 min at 55 °C and 90 s at 72 °C, followed by 10 min at 72 °C. All primers were tagged with the Illumina adapter sequences (TCG TCG GCA GCG TCA GAT GTG TAT AAG AGA CAG and GTC TCG TGG GCT CGG AGA TGT GTA TAA GAG ACA G) allowing the construction of amplicon libraries by a two-step PCR. Additionally, DNA extraction was carried out without any biological matrix and was considered a negative control to evaluate ambient and kit products contamination. Amplification signals were verified by electrophoresis on agarose gel 1.5%. High-throughput sequencing was achieved after pooling PCR triplicates using Illumina MiSeq (2 × 300 bp, paired-end chemistry v3), and was performed by Microsynth (Balgach, Switzerland), aiming (for each sample) at 40,000 sequences for the bacterial 16 S rRNA gene, the 18 S rRNA gene, and 70,000 sequences for the archaeal 16 S rRNA gene.

For each dataset i.e. bacterial 16 S rRNA genes, archaeal 16 S rRNA genes and 18 S rRNA genes, paired-ends reads obtained were demultiplexed in the samples according to exact match adaptors (removed) and reads were merged with a maximum of 10% mismatches in the overlap region using FLASh (Magoč and Salzberg, 2011). Denoising procedures was carried out by discarding reads without the expected length (200–500 bp) or containing any ambiguous base (N). After dereplication of sequences, clusterization was performed using SWARM (Mahé et al., 2014), which uses a local clustering threshold (rather than a global clustering threshold) and an aggregation distance of 3 for identification of operational taxonomic units (OTUs). The lower taxonomic level reached to define OTUs corresponded to (depending on taxa considered) the genus or the species ('genus/species' level). Chimeric sequences were discarded using VSEARCH (Rognes et al., 2016), and low-abundance sequences were filtered at 0.005% of all sequences. Taxonomic affiliation was preformed with both RDP Classifier and BLASTn (Zhang and Madden, 1997) against the 138.1 SILVA database (Quast et al., 2013) for bacteria, archaea and microeukaryotes, which was automated in the FROGS pipeline (Escudié et al., 2018). Contaminant OTUs identified from the negative controls (blank samples) were removed and the eukaryotic dataset was manually curated for metazoan sequences (data not shown). To compare samples, a normalization procedure was applied by randomly resampling down to 15,196, 1220 and 25,646 sequences in the bacterial, archaeal and microeukaryotic 18 S data sets, respectively.

### 2.3. Statistical analyses

Rarefaction curves were calculated to assess sequencing efficacy, using Paleontological Statistics (PAST) software v4.02 (Hammer et al., 2001). OTU richness and diversity were estimated using Chao 1 index (Chao, 1987), Shannon's H' (Shannon, 1948), Evenness $E^{H/S}$ index (Harper, 1999) and Simpson (1-D) index (Simpson, 1949), as previously described (Bontemps et al., 2023). Communities were compared with NMDS, using VEGAN package in R v4.0.2 (R Core Team, 2020). Analysis of similarity (ANOSIM) was conducted using the VEGAN package in R, to test differences ($P < 0.05$) in overall community composition between

different sampling conditions (see above) and to further confirm the results observed in the NMDS plot. A Bonferroni correction was applied on *P* values to lower alpha risk. All analyses were based on similarity matrices calculated with the Bray-Curtis similarity index (Bray and Curtis, 1957), using R.

A central emphasis in this study was to verify the effects of cleaning method and time (i.e., succession) on the microbiome. To analyze the whole dataset with different experimental designs and focus on these effects, the axis 1 of NMDS was regressed with a generalized linear mix model (GLMM) using the 'lem4' package in R. The models explain the target axis value according to time, cleaning method and their interactions.

## 3. Results

### 3.1. Contaminants associated to cleaning tools

The scalpels used for cleaning were sterile, but not the sponges. Analysis of sponges prepared for cleaning operations evidenced 199 bacterial OTUs, 10 archaeal OTUs and 103 microeukaryotic OTUs. Bacterial OTUs belonged mainly to the phylum Proteobacteria (102 OTUs) followed by Actinobacteria (51 OTUs) and Myxococcota (8 OTUs). All 10 archaeal OTUs were affiliated to the phylum Thaumarchaeota. The microeukaryotic OTUs belonged mainly to the phylum Ascomycota (83 OTUs), followed by the Mucoromycota (8 OTUs). These taxa have the potential to represent useful indicators of cave contamination.

### 3.2. Visual dynamics upon stain cleaning

The visual aspect of black stains and unmarked surfaces did not change during the 19-month study. Mechanical cleaning of black stains was effective to removed black constituents, leading to a surface visually similar to unmarked surfaces located nearby (Supplementary Materials, Fig. S1). Essentially no change in visual properties was identified at 3 weeks and 4 months after cleaning. At 16 and 19 months after cleaning, black stains had not reformed, but (i) cleaned areas had became heterogeneous, with the appearance of darker spots, visible mainly using a Dinolite microscope (Supplementary Materials, Fig. S2GH) and (ii) a black border, thin and discontinuous (which was preferentially sampled at 16 and 19 months), had started forming at the periphery of several of them, following the shape of the 'old stain' (Supplementary Materials, Fig. S2CD).

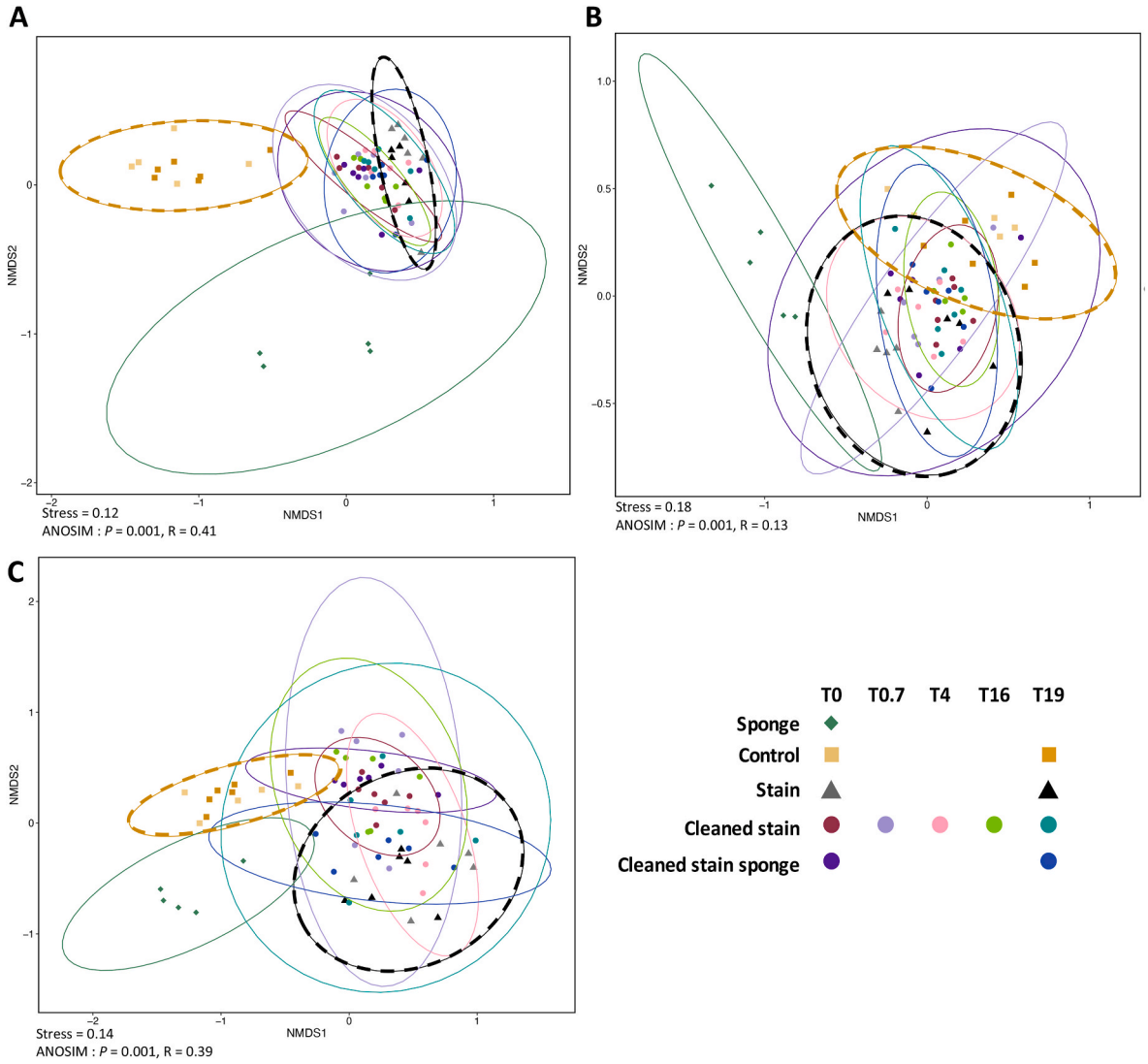


**Fig. 2.** Non-metric MultiDimensional scaling (NMDS) analysis of microbial community structure in Lascaux's Cave according to rock surface condition and time. Ellipse (95% confidence interval) indicate the different rock surface condition for bacteria (A), archaea (B) and microeukaryotes (C). Controls conditions are represented with dotted circle. 'Cleaned stain ': black stain cleaned with a scalpel only; 'Cleaned stain sponge': black stain cleaned with a scalpel and then a sponge.

### 3.3. Community structure

NMDS and ANOSIM analyses indicated that the effect of rock surface condition (i.e. stain, stain after cleaning, or unstained surface × cleaning method if applicable × sampling time) on community structure was significant for bacteria ($P = 0.001$, $R^2 = 0.55$, Fig. 2A and Supplementary Materials, Table S2), archaea ($P = 0.001$, $R^2 = 0.32$, Fig. 2B and Supplementary Materials, Table S3) and microeukaryotes ($P = 0.001$, $R^2 = 0.44$, Fig. 2C and Supplementary Materials, Table S4). In particular, data showed that black stain cleaning has a significant effect on the bacterial ($P = 0.001$, $R^2 = 0.13$) and microeukaryotic communities ($P = 0.001$, $R^2 = 0.11$), but not the archaeal community ($P = 0.34$,

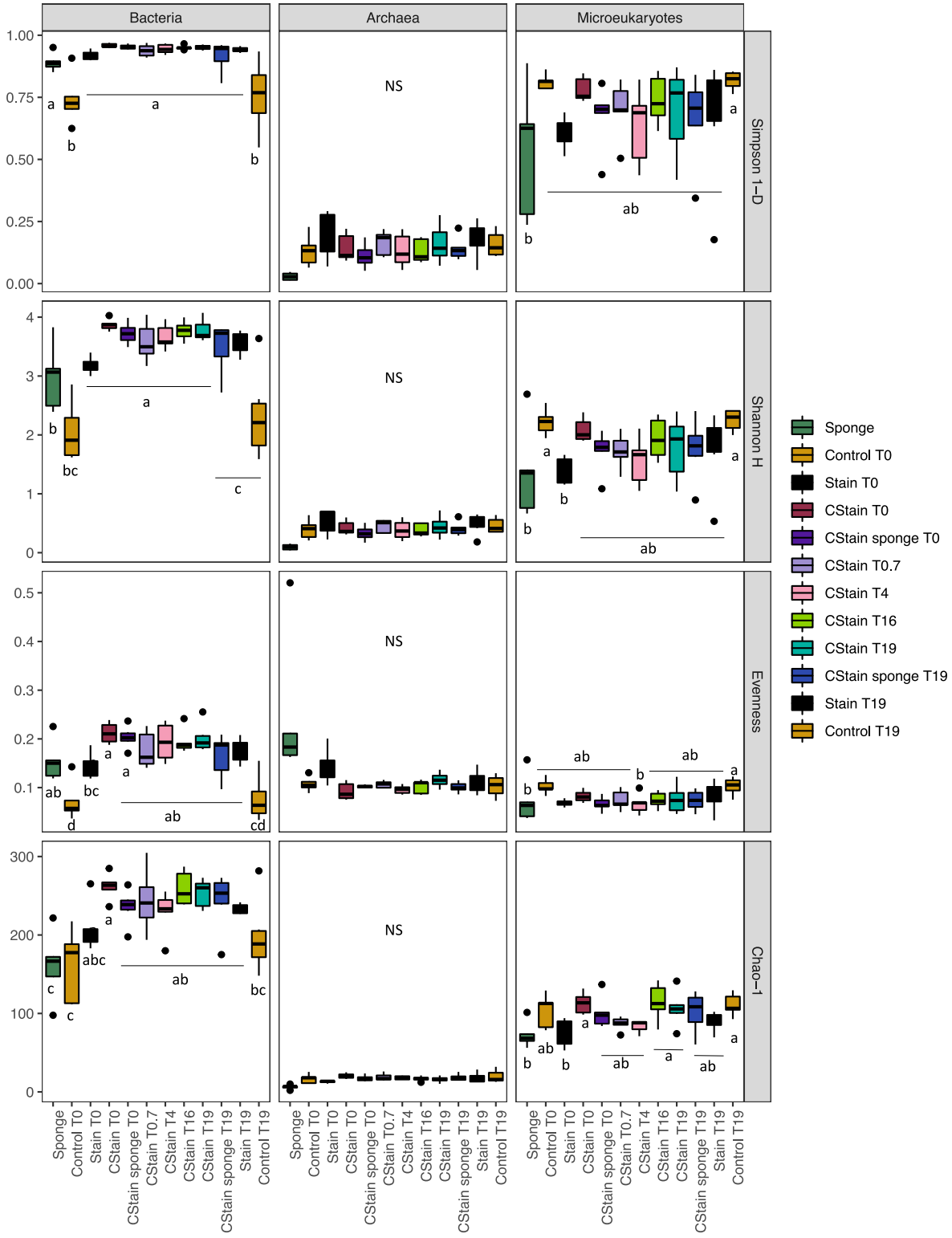


**Fig. 3.** Alpha diversity indices of microbial community according to rock surface condition, based on estimated evenness (Evenness index), richness (Chao-1 index) and diversity (Simpson 1-D index and Shannon H′ index). For each domain of life, significant differences between surface conditions are shown with letters (Wilcoxon tests, $P < 0.05$).

$R^2 = 0.03$). In this context, there was no difference between cleaning methods (i.e scapel vs scalpel/sponge) at T0, for bacteria ($P = 0.89$, $R^2 = 0.05$), archaea ($P = 0.39$, $R^2 = 0.10$) and microeukaryotes ($P = 0.38$, $R^2 = 0.10$).

Afterwards, the effect of recolonization time on community structure (i.e., using only samples from surfaces that underwent cleaning) was significant for bacteria ($P = 0.036$) and microeukaryotes ($P = 0.04$), but not for archaea ($P = 0.34$) (Supplementary Materials, Fig. S3). Moreover, the interaction between recolonization time and cleaning method was significant with the scalpel/sponge cleaning method ($P = 0.03$ and $R^2 = 0.72$ for bacteria, $P = 0.02$ and $R^2 = 0.56$ for microeukaryotes) but not with the scalpel cleaning method ($P = 0.1$ and $R^2 = 0.72$ for bacteria, $P = 0.86$ and $R^2 = 0.56$ for microeukaryotes) (Supplementary Materials, Fig. S3).

### 3.4. Microbial richness and diversity levels

For bacteria, Chao-1 richness index, Simpson 1-D and Shannon H′ diversity indices were lower for control conditions (Control T0 and Control T19 samples) than (i) all other rock surface conditions for Simpson 1-D (Wilcoxon test: $P = 1.9 \times 10^{-5}$ and $P = 3.1 \times 10^{-4}$, respectively) and Chao-1 ($P = 7.3 \times 10^{-5}$ and $P = 2.2 \times 10^{-4}$, respectively), or (ii) most other rock surface conditions (for Shannon H'; $P = 0.002$ and $P = 0.001$, respectively), without any effect of cleaning or recolonization time (Fig. 3). The evenness diversity index was higher for cleaned surface conditions at T0 (CStain T0 and CStain sponge T0 samples) than for the other rock surface conditions ($P = 1.5 \times 10^{-4}$ and $P = 1.7 \times 10^{-4}$, respectively), therefore the effects of cleaning and of recolonization time were significant based on this criterion, and for both effects it was without a difference between cleaning methods.

For archaea, the differences in Chao-1 richness index, Simpson 1-D and Shannon H' diversity indices, and Evenness diversity index between rock surface conditions were not significant (Fig. 3), pointing to a lack of effect of cleaning and of recolonization time.

For microeukaryotes, differences in Simpson 1-D diversity index between rock surface conditions were not significant, whereas Shannon index was higher for control conditions (T0 and T19 samples) than all other rock surface conditions ($P = 0.001$ and $P = 4.5 \times 10^{-4}$, respectively) (Fig. 3). Chao-1 index for black stains at T0 (Stain T0 samples) and Evenness index for cleaned surfaces at 4 months (CStain T4 samples) were lower than for the other rock surface conditions ($P = 1.1 \times 10^{-4}$ and $P = 0.001$, respectively). Thus, there was some impact of black stain cleaning (for both cleaning methods) but essentially none of recolonization time.

### 3.5. Microbial community composition in black stains vs unmarked surfaces

Unmarked surfaces (control) had similar bacterial, archaeal and microeukaryotic communities (Pairwise Adonis: $P = 0.882$, $R^2 = 0.4$; $P = 0.479$, $R^2 = 0.08$ and $P = 0.325$, $R^2 = 0.12$, respectively) across time (T0 vs T19) (Supplementary Materials, Tables S3, S4 and S5). The bacterial community was composed of 19 classes with predominantly Gammaproteobacteria (82.4% of bacterial sequences), highly represented by the *Pseudomonas* genus (73.9%) following by Alphaproteobacteria (9.9%) and Actinobacteria (2.3%) (Figs. 4A and 5A). Archaeal community composition was characterized by the dominance of the Nitrososphaeria class (100% of archaeal sequences) (Fig. 4B). The microeukaryotic community was composed of 21 classes including Sordariomycetes (43.0% of microeukaryotic sequences), Leotiomycetes (18.7%) mostly affiliated to the *Pseudogymnoascus* genus (18.3%) and Dothideomycetes (7.9%) (Figs. 4C and 5B).

Black stains had similar bacterial, archaeal and microeukaryotic communities (Pairwise Adonis: $P = 0.386$, $R^2 = 0.10$; $P = 0.198$, $R^2 = 0.13$ and $P = 0.766$, $R^2 = 0.04$, respectively) across time (T0 vs T19) (Supplementary Materials, Tables S3, S4 and S5). The bacterial community of black stains was composed of 19 classes including Alphaprotebacteria (37.4%), Actinobacteria (18.6%), Bacteroidia (16.8%) highly represented by the *Chitinophaga* genus (8.2%) and Acidobacteriae (12.9%) mostly affiliated to the *Bryobacter* genus (12.2%) (Figs. 4A and 5A). The archaeal community was composed of the two classes Nitrososphaeria (97.6%) and Halobacterota (2.4%) (Fig. 4B). The microeukaryotic community consisted in 19 classes with predominantly the Eurotiomycetes class (65.9%) and especially the *Exophiala* genus (25.4%), followed by Sordariomycetes (21.0%) and Dothideomycetes (1.7%) (Figs. 4C and 5B).

Unmarked surfaces showed significant differences compared with black stains for bacterial (whatever the sampling time), archaeal and microeukaryotic communities (Supplementary Materials, Tables S3, S4 and S5). For the three domains of life, community composition showed strong variations between stained and unmarked surfaces for the most abundant classes or genera, notably for the Gammaproteobacteria (an average of −72% in black stains compared with unstained surfaces based on T0 and T19 data), Alphaproteobacteria (+28%), Bacteroidia (−15%), Sordaryomycetes (−22%), Leotiomycetes (−19%) and Eurotiomycetes (+59%) classes (Fig. 4AC). Similarly, strong variations were also observed at genus level, especially for *Pseudomonas* (an average of −74% in black stains compared with unstained surfaces), *Chitinophaga* (+6%), *Pseudogymnoascus* (−18%) and *Exophiala* genera (+24%) (Fig. 5).

### 3.6. Relative abundance of taxa after scalpel cleaning and across recolonization states

Scalpel cleaning of black stains changed microbial community composition for bacteria and microeukaryotes, as the relative abundance of bacteria *Nonomuraea* and fungi *Exophiala* and *Ochroconis* amounted to respectively 5.9%, 24.3% and 0.8% in stained surfaces vs 2.4%, 9.8% and 10% in cleaned surfaces (Fig. 5). Cleaning had resulted in removal of black surface constituents, but without reaching the community composition of unmarked surfaces, as for instance *Luteimonas* reached 9.0% on cleaned surfaces, *Nocardioides* 5.7% and *Chitinophaga* 18.0%, vs only 0.1%, 0.07% and 0.7%, respectively, in unmarked surfaces.

Immediately after cleaning, microbial communities were mainly composed of Alphaproteobacteria, Actinobacteria, Nitrososphaeria and Sordariomycetes classes (Fig. 4), but community composition changed during the next 19 months for bacteria and microeukaryotes (Supplementary Materials, Tables S3, S4 and S5). In the bacterial community, the relative abundance of the gammaproteobacterial class (mainly the *Pseudomonas* genus) decreased from 15.2% of sequences to 6.7% (and *Pseudomonas* from 5.6% to 0.9%) between T0 and T19 (Figs. 4A and 5A). The Chloroflexia and Planctomycetota bacterial classes (about 0.6% and 0.5% from T0 to T16, respectively) increased in relative abundance to 5.8% and 7.8%, respectively, at T19 (Fig. 4A). The Actinobacteria class reached 17.5% at T0 and T0.7, 24.5% at T4 but only 12.7% at T16 and T19. At genus level, *Luteimonas* and *Nocardioides* genera amounted to respectively 3.3% and 3.0% at T0 and T0.7, 9.3% at T4, but only 1.6% and 1.7% at T16 and T19 (Fig. 5A), whereas *Chitinophaga* increased from 9.9% (at T0, T0.7 and T4) to 18.5% (at T16 and T19) and *Pedomicrobium* decreased from 8.9% (at T0, T0.7 and T4) but to about 4.1% (at T16 and T19).

In the microeukaryotic community, the Sordariomycetes reached a relative abundance of 50.4% at T0, T0.7, T4 and T16, but only 38.0% at T19 (Fig. 4C). The relative abundance of Dothideomycetes and Eurotiomycetes fluctuated, as the Dothideomycetes reached 11.7% at T0, 14.0% at T0.7, 6.4% at T4, 13.3% at T16 and 9.6% at T19, whereas the Eurotiomycetes amounted to 36.6% at T0, 25.1% at T0.7, 38.1% at T4, 26.3% at T16 and 41.1% at T19. At genus level, *Exophiala* was stable (8.9–11.2%), *Ochroconis* fluctuated (10.9% at T0, 13.8% at T0.7, 6.3% at T4, 6.4% at T16 and 6.5% at T19), and *Capronia*, *Conidiobolus* and Unidentified genera amounted to 19.1%, 2.6% and 47.2% at T0, T0.7, T16

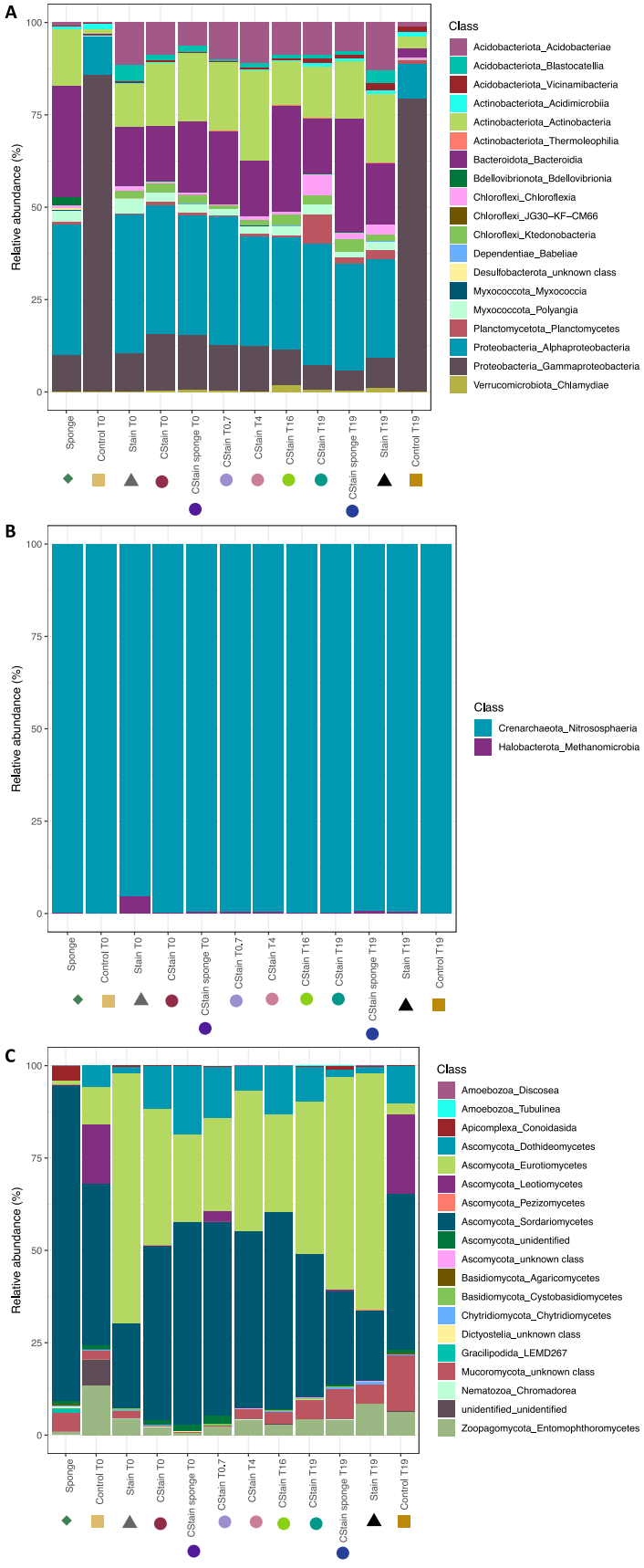


**Fig. 4.** Relative abundance (% of sequences) of bacterial (A), archaeal (B) and microeukaryotic (C) classes according to rock surface condition. The symbols represent each surface condition studied, as used in Fig. 2.

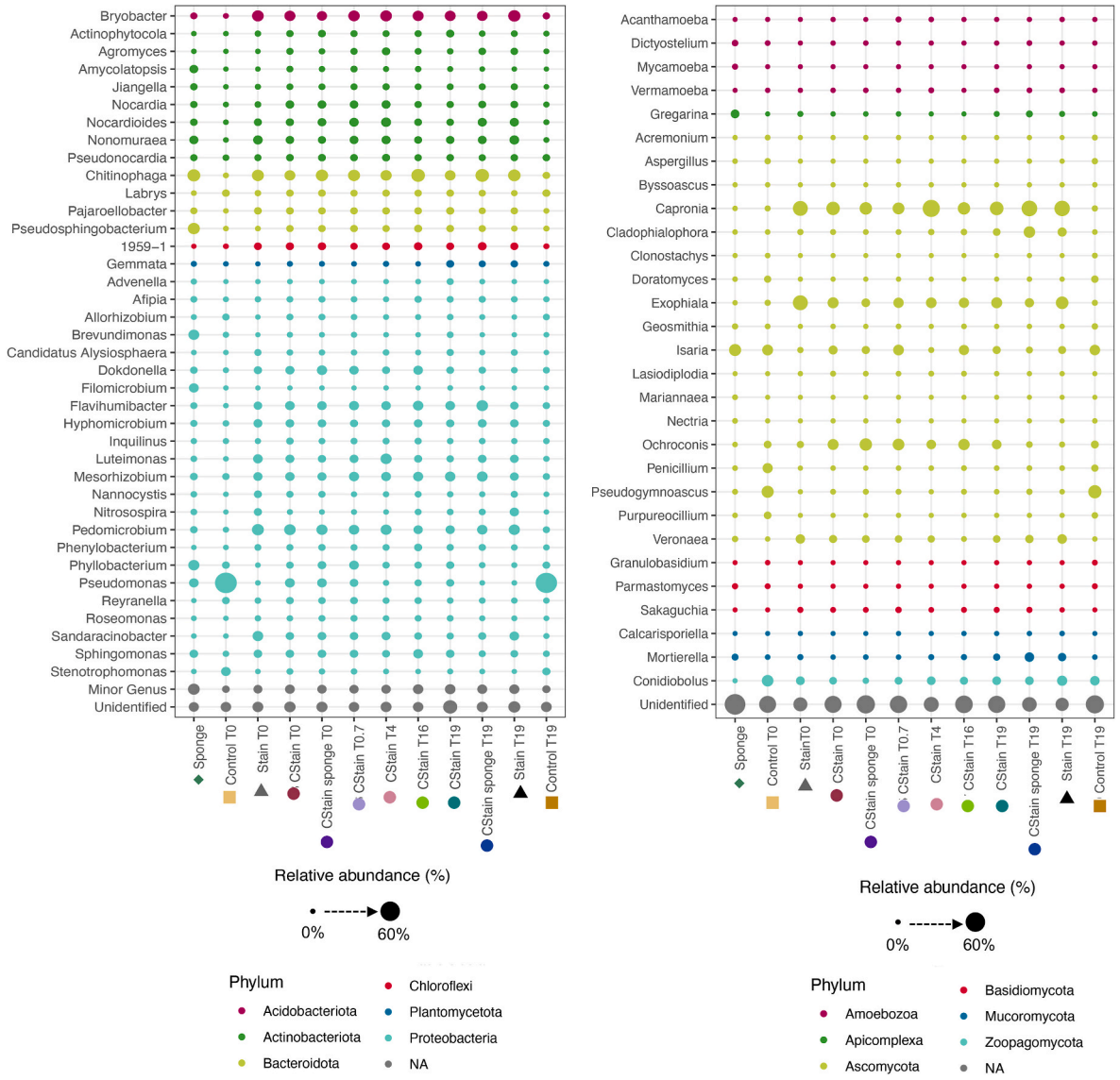


**Fig. 5.** Distribution of the most abundant bacterial (A) and microeukaryotic (B) genera according to rock surface condition or sponge (also indicated with the symbols used in Figs. 2 and 4). Within the panel, the relative abundance of the genera is proportional to the diameter of the circles, all genera of relative abundance <0.05% of total normalized sequences were considered as minor genera, and the color of the circles represents the taxonomic affiliation at phylum level.

and T19 but at T4 they reached 46.1%, 4.3% and 30.6%, respectively (Fig. 5B).

### 3.7. Cleaning method comparison

Unlike the bacterial community (Fig. 4A), class composition of the fungal community immediately after cleaning depended on the cleaning method (Fig. 4C). The Dothideomycetes reached a relative abundance of 11.7% (scalpel) versus 18.5% (scalpel/sponge), whereas the Eurotiomycetes amounted to 36.6% (scalpel) vs 23.6% (scalpel/sponge) and the Sordariomycetes 47.3% (scalpel) vs 54.9% (scalpel/sponge). These contrasted abundances were also visible at the genus level, as *Exophiala* and *Ochroconis* amounted to 11.2% and 11.0% (scalpel) vs 4.0% and 17.2% (scalpel/sponge), respectively (Fig. 5B). At that level, some differences were seen also with bacteria, e.g. with *Chitinophaga* at 13.0% (scalpel) vs only 8.3% (scalpel/sponge) (Fig. 5A).

At 19 months after cleaning (T19), the Bacteroidota amounted to a relative abundance of 15.0% (scalpel cleaning) versus as much as 30.6% where scalpel and sponge had been used (Fig. 4A), and the Chloroflexia reached 5.8% (scalpel) vs 1.8% (scalpel/sponge). The Dothideomycetes class accounted for 9.5% of sequences (scalpel) vs only 1.9% (scalpel/sponge) and the Sordariomycetes for 38.6% (scalpel) vs only 25.3% (scalpel/sponge) (Fig. 4C), whereas the Eurotiomycetes amounted to 41.1% (scalpel) vs 57.7% (scalpel/sponge). At genus level, *Pedomicrobium* amounted to 4.0% (scalpel) and 6.9% (scalpel/sponge) (Fig. 5A), whereas *Chitinophaga* reached 18.8% (scalpel) vs only 8.0% (scalpel/sponge) and *Phyllobacterium* 2.0% (scalpel) vs only 0.4% (scalpel/sponge), and *Flavihumibacter* amounted to 5.2% (scalpel) vs as much as 10.7% (scalpel/sponge). *Exophiala* and *Ochroconis* amounted to 10.9% and 6.4% (scalpel) vs only 5.4% and 0.7% (scalpel/sponge), respectively (Fig. 5B). In contrast, *Capronia, Cladophialophora* and *Veronaea* reached 23.2%, 2.1% and 1.9% (scalpel) vs as much as 35.4%, 13.2% and 3.4% (scalpel/sponge), respectively.

### 3.8. Fate of microbial contaminants from sponge

Microbial OTUs present in sponge samples but not in black stain or unstained surfaces were mainly affiliated to Bacteroidia (OTU_617), Alphaproteobacteria (OTU_65 = *Brevundimonas*) and Sordariomycetes class (i.e. OTU_332 = *Isaria* and OTU_455 = *Nectria*), while other sponge

OTUs were also present in black stains or unstained surfaces, i.e. Acidimicrobiia (OTU_627, OTU_251), Bacteroidia (OTU_246, OTU_259, OTU_245), Alphaproteobacteria (OTU_981, OTU_810 = *Filomicrobium*, OTU_441), Planctomycetes (OTU_1027), Eurotiomycetes (OTU_19, OTU_3, OTU_14), Enthromophtoromycetes (OTU_6), Sordariomycetes (OTU_24, OTU_7, OTU_8), etc. (Fig. 6).

When the comparison was widened to include scalpel-cleaned surfaces, it appeared that OTUs found in sponge and sponge-cleaned samples at T0 and T19 but not in black stains, unstained surfaces or scalpel-cleaned stains were OTU_582 (unidentified Planctomycete), OTU_747 (unidentified Gammaproteobacteria), OTU_106 (*Veronaea*, Eurotiomycetes), OTU_488 (unidentified Eurotiomycete), OTU_304 (*Isaria*, Sordariomycete) and OTU_354 (unidentified Sordariomycete) (Fig. 6). Overall, these OTUs indicative of contamination represented respectively 0.15% and 0.08% (at T0) and 0.10% and 0.10% (at T19) of the bacterial and microeucaryotic sequences in sponge-cleaned samples. In addition, OTU_432 affiliated to *Cephalotrichum* genus (Sordariomycetes) and associated with sponge was also present in scalpel-cleaned stain at T4 (Fig. 6B).

On the first day of the study, taxa evidenced in sponges corresponded to 89% and 96% of the bacteria and microeucaryota sequences, respectively, on surfaces immediately after scalpel/sponge cleaning, vs 88% and 97% in black stains, 81% and 97% on unmarked surfaces and 86% and 96% on surfaces immediately after scalpel cleaning. Overall, these taxa present on sponges corresponded, at 19 months, to 90% and 98% of the bacteria and microeucaryota sequences, on surfaces that had undergone scalpel/sponge cleaning, vs 86% and 96% in black stains, 82% and 98% on unmarked surfaces and 82% and 96% on surfaces that had been cleaning with scalpel only. This means that taxa present on sponges were already well represented on Lascaux surfaces.

## 4. Discussion

Mechanical cleaning of stains is a routine procedure in show caves. We aimed at testing the hypothesis that mechanical cleaning of black stains would lead to a pioneer-like community likely to undergo further microbial dynamics and perhaps microbial successions leading to the reformation of black stains, using the UNESCO cave of Lascaux. NMDS and Adonis analysis showed that the microbial communities of black stains and unstained surfaces differed significantly from each other and were stable. This parallels the stability of cave environmental conditions (Bourges et al., 2014; Di Russo et al., 1997; Engel and Northup, 2008) and especially the stability of black stains (once formed) in this part of the cave. Black stains in the Absidiole displayed counter-selection of *Pseudomonas* bacteria (from 73.9% of bacterial sequences to 0.03%) and selection of *Exophiala* fungi (from 0.4% to 30.4% of fungal sequences), as in Lascaux's Passage (Alonso et al., 2018), but surprisingly the relative abundance of *Ochroconis* fungi was of the same level in unmarked and stained surfaces (an average of 2%). *Exophiala* fungi have been found in environments rich in aromatic compounds (i.e. arsenic mine, creosote-treated wood and soil contaminated with aromatic hydrocarbons), where they can use alkybenzene as the sole carbon source (Cox et al., 1993; Zhao et al., 2010). Also, these fungi have the potential to produce melanin pigment, which gives this black color to the stains in tombs (Isola et al., 2021) or caves (Martin-Sanchez et al., 2012; Alonso et al., 2023). Thus, selection of *Exophiala* black fungi was likely to have been promoted by the availability of residues of aromatic biocides used at Lascaux (Martin-Sanchez et al., 2015).

Against this background, mechanical cleaning of black stains with sterile scalpels resulted in a richer community (with 462 taxa instead of 383), probably because dominant taxa were trimmed during stain removal. It was not the same community as in neighboring unmarked surfaces, even though the surface was not black anymore. Immediately after scalpel cleaning, the microbial community was mainly composed of Alphaproteobacteria, Actinobacteria, Nitrososphaeria and Sordariomycetes classes, and the relative abundance of *Pedomicrobium*, *Ochroconis*, *Pseudomonas* genera was significant.

The community thus obtained by scalpel cleaning was not stable, as microbial changes took place subsequently. Indeed, NMDS axis-1 values were significantly associated with recolonization time (Supplementary Materials, Fig. S3), pointing that the cleaning experiment induced a microbial succession on the wall. Early successional stages are expected to include r-strategy taxa (Odum, 1969), with fast growth, high turnover rates and copiotrophy, which promote colonization (Barbault, 1995; Zhou and Ning, 2017). This is the case of many Proteobacteria, such as *Pseudomonas* (Jurburg et al., 2017). Early taxa may change surface conditions and facilitate microbial successions (Boston et al., 2009; Uroz et al., 2009). In Lechuguilla Cave (New Mexico), pioneer microorganisms (unidentified) produce organic acids that promote dissolution of cemented bedrock (Northup, 1997; Spilde et al., 2005). Here, microbial succession was observed only for bacterial and microeukaryotic communities, over the 19 months following cleaning. Several patterns of microbial dynamics were observed, i.e. (i) a linear decrease in relative abundance from T0 to T19, for instance for Gammaproteobacteria and mainly the *Pseudomonas* genus, (ii) a decrease from T4 to T19 (for *Ochroconis*), (iii) stable abundance from T0 to T19 (e.g. for *Exophiala*), (iv) stable abundance with a peak only at T4 (for *Luteimonas, Nocardioides* and *Capronia*), and (v) an increase from T4 to T19 (for *Chitinophaga*, Dothideomycetes). Thus, most changes are observed at 4 months and after, with the selection of certain taxa that could correspond to K-strategy species. This is the case of many Actinobacteria (Bastian et al., 2009c). After the initial stages of colonization, K strategists with high competitive ability are expected to be preferentially selected (Yin et al., 2022).

Microbial communities 19 months after scalpel cleaning were not yet similar to those of black stains, with *Chitinophaga* at a relative abundance of 18% (vs 8% in black stains) and the black fungus *Ochroconis* at 10% vs 0.8%. This was not surprising, as the original black stains as such did not reform. Perhaps black stains reformation requires other pigmented taxa. Black stains in the Apse typically display *Folsomia candida* collembola, which can feed on black fungi and disseminate them (Alonso et al., 2023; Bastian et al., 2009a). These collembola were back within weeks of stain cleaning in 2015 but were sparsely seen in this work, suggesting that melanin synthesis may be a response to grazing. Monitoring of *F. candida* populations in various areas of the cave showed that their dynamics can be erratic (personal communication from S. Géraud). Here, the microbial community on cleaned surfaces did not change much between 16 and 19 months, pointing that secondary succession could lead to a paraclimax. Microbial recolonization depends on the disturbance regime, microbial legacy and microbial dynamics related to species regrowth, immigration and recruitment (Cox et al., 1993; Zhao et al., 2010).

In addition to representing a useful experimental approach to generate artificially a pioneer community for subsequent monitoring, this experiment was also based on the rationale that mechanical cleaning is a routine procedure followed by restorers to remove stains in show caves as well as historical buildings. Various mechanical cleaning techniques can have a negative impact on the conservation of cave paintings (He et al., 2022). For example, scalpels cause physical damage to the walls, cotton swabs can push certain spores and mycelium into the surface microstructure and cause contamination over larger areas. However, no studies have investigated the effects of mechanical cleaning carried out with scalpels or scalpels/sponges, despite the use of these procedures for restoration of ancient artwork. Therefore, we included a standard cleaning procedure in which sponges are also used, for stain removal and final smoothing of cleaned surfaces. Here, however, we showed that sponges, despite disinfection in boiling water, displayed a microbial community of their own. Three issues are raised. First, as expected, this community differed from that of rock surface conditions in Lascaux, but it included Bacteroidota, which have been proposed as bioindicators of anthropization in caves (Alonso et al., 2018; Pfendler et al., 2018) as well as the black fungus *Exophiala*. This raises the


**Fig. 6.** Occurrence of all bacterial (A) and microeukaryotic OTUs (B) according to rock surface condition or sponge. OTU codes are shown in the outer circle, while phyla affiliation is shown in the inner circle. OTU presence is indicated in dark blue. Taxa names for OTU codes are listed in Supplementary Materials, Table S6.

possibility that allochthonous strains from these taxa could actually contribute to cave populations following routine cleaning procedures. Second, some taxa present on the sponge were found only on surfaces cleaned with the sponge, pointing to microbial contamination via the sponge (but at modest levels of relative abundance). This is the case of the bacterial genus *Filomicrobium* and fungal genera *Isaria* and *Cephalotrichum*, which have been also identified in other anthropized subsurface environments (Diaz-Herraiz et al., 2014; Miller et al., 2020). These microorganisms might be significant for cave conservation issues, as *Filomicrobium* and *Cephalotrichum* were pointed at in biodegradation of respectively the Tomba del Coll Etruscan tomb (Diaz-Herraiz et al., 2014) and the Takamatsuzuka Tumulus stone chamber in Japan (Kiyuna et al., 2017), but here scalpel/sponge cleaning did not lead to darker surfaces than scalpel cleaning at 19 months. Therefore, cosmopolitan taxa with surface alteration potential may be disseminated during cleaning procedures, and more care is needed when selecting these procedures for cultural heritage sites. Third, the sponge treatment can modify rock surface properties, selecting certain species with particular adhesion properties and able to thrive (Barton and Jurado, 2007; Uroz et al., 2015). This may also contribute to changes in microbial community composition. Overall, the GLMM model, in which the NMDS axis 1 was explained by recolonization time, the cleaning method, and their interactions, showed microbiome shifts over time (i.e., from smaller to larger axis-1 values for bacteria, and from larger to smaller axis-1 values for microeukaryotes). Such community shifts documented based on NMDS axis-1 data were more significant with the scalpel/sponge method ($P < 0.05$), suggesting stronger microbial dynamics after this cleaning method compared with the scalpel method.

## 5. Conclusion

Rock surface alterations by microorganisms in Paleolithic caves are of high concern for conservation of artwork, and here we show that mechanical cleaning of black stains leads to subsequent microbial successions. Early recolonization involved specific taxa e.g. *Pseudomonas*, *Pedomicrobium* and black-melanized fungi *Ochroconis*, followed by *Chitinophaga* members of the Dothideomycetes class, probably leading to a paraclimax. Thus this type of cleaning may prompt further alterations. In addition, we showed that the use of sponge for mechanical cleaning, a routine procedure in restoration of heritage sites, can have a significant impact on microbial communities and contribute to contamination of cave surfaces by microorganisms with bioalteration potential. Thus, our work provides a better understanding of microbial dynamics associated with surface alterations in Paleolithic caves and identifies potential contamination and microbial recolonization indicators. It also highlights shortcomings in current conservation procedures used in Paleolithic caves, geological show caves visited for outstanding speleothems, as well as underground heritage sites such as catacombs etc.

## CRediT authorship contribution statement

**Zélia Bontemps:** Writing – original draft, Visualization, Resources, Methodology, Investigation, Formal analysis. **Mylène Hugoni:** Writing – original draft, Validation, Supervision, Methodology. **Yvan Moënne-Loccoz:** Writing – original draft, Validation, Supervision, Project administration, Methodology, Investigation, Funding acquisition, Conceptualization.

## Declaration of competing interest

The authors declare that they have no known competing financial interests or personal relationships that could have appeared to influence the work reported in this paper.

## Data availability

Data will be made available on request.

## Acknowledgements

We thank S. Géraud, J.C. Portais, M. Mauriac (DRAC Nouvelle Aquitaine) and D. Henry-Lormelle (restorer team) for information and help, and Lascaux Scientific Board for useful discussions. Funding was provided by DRAC Nouvelle Aquitaine (Bordeaux, France).

## Appendix A. Supplementary data

Supplementary data to this article can be found online at https://doi.org/10.1016/j.ibiod.2024.105797.

## References

Alabouvette, C., Saiz-Jiménez, C., 2011. Écologie microbienne de la Grotte de Lascaux. CSIC-Instituto de Recursos Naturales y Agrobiología de Sevilla (IRNAS).
Alonso, L., Creuzé-des-Châtelliers, C., Trabac, T., Dubost, A., Moënne-Loccoz, Y., Pommier, T., 2018. Rock substrate rather than black stain alterations drives microbial community structure in the passage of Lascaux Cave. Microbiome 6, 216.
Alonso, L., Pommier, T., Simon, L., Maucourt, F., Doré, J., Dubost, A., Trân Van, V., Minard, G., Valiente Moro, C., Douady, C.J., Moënne-Loccoz, Y., 2023. Microbiome analysis in Lascaux Cave in relation to black stain alterations of rock surfaces and collembola. Environ. Microbiol. Rep. 15, 80–91.
Barbault, R., 1995. Biodiversity dynamics: from population and community ecology approaches to a landscape ecology point of view. Landsc. Urban Plann. 31, 89–98.
Barton, H.A., Jurado, V., 2007. What's up down there? Microbial diversity in caves microorganisms in caves survive under nutrient-poor conditions and are metabolically versatile and unexpectedly diverse. Microbes 2, 132–138.
Bastian, F., Alabouvette, C., Saiz-Jimenez, C., 2009a. The impact of arthropods on fungal community structure in Lascaux Cave. J. Appl. Microbiol. 106, 1456–1462.
Bastian, F., Alabouvette, C., Jurado, V., Saiz-Jimenez, C., 2009b. Impact of biocide treatments on the bacterial communities of the Lascaux Cave. Naturwissenschaften 96, 863–868.
Bastian, F., Bouziri, L., Nicolardot, B., Ranjard, L., 2009c. Impact of wheat straw decomposition on successional patterns of soil microbial community structure. Soil Biol. Biochem. 41, 262–275.
Bastian, F., Jurado, V., Nováková, A., Alabouvette, C., Saiz-Jimenez, C., 2010. The microbiology of Lascaux cave. Microbiology 156, 644–652.
Bernardini, S., Bellatreccia, F., Columbu, A., Vaccarelli, I., Pellegrini, M., Jurado, V., Del Gallo, M., Saiz-Jimenez, C., Sodo, A., Millo, C., Jovane, L., De Waele, J., 2021. Morpho-mineralogical and bio-geochemical description of cave manganese stromatolite-like patinas (Grotta del Cervo, Central Italy) and hints on their paleohydrological-driven genesis. Front. Earth Sci. 9, 642667.
Bontemps, Z., Hugoni, M., Moënne-Loccoz, Y., 2023. Microscale dynamics of dark zone alterations in anthropized karstic cave shows abrupt microbial community switch. Sci. Total Environ. 862, 160824.
Boston, P.J., Spilde, M.N., Northup, D.E., Curry, M.D., Melim, L.A., Rosales-Lagarde, L., 2009. Microorganisms as speleogenetic agents: geochemical diversity but geomicrobial unity. In: Klimchouk, A.B., Ford, D.C. (Eds.), Hypogene Speleogenesis and Karst Hydrogeology of Artesian Basins. Ukrainian Institute of Speleology and Karstology, Chernivtsi, Ukraine, pp. 51–58.
Bourges, F., Genthon, P., Genty, D., Lorblanchet, M., Mauduit, E., D'Hulst, D., 2014. Conservation of prehistoric caves and stability of their inner climate: lessons from Chauvet and other French caves. Sci. Total Environ. 493, 79–91.
Bray, J., Curtis, J., 1957. An ordination of the upland forest communities of southern Wisconsin. Ecol. Monogr. 27, 325–349.
Chalmin, E., d'Orlyé, F., Zinger, L., Charlet, L., Geremia, R.A., Orial, G., Menu, M., Baffier, D., Reiche, I., 2007. Biotic versus abiotic calcite formation on prehistoric cave paintings: the Arcy-sur-Cure 'Grande Grotte' (Yonne, France) case. Geol. Soc. London 279, 185–197. Special Publications.
Chao, A., 1987. Estimating the population size for capture-recapture data with unequal catchability. Biometrics 43, 783–791.
Cigna, A., 2016. Tourism and show caves. Geomorphology 60, 217–233.
Cox, H.H.J., Houtman, J.H.M., Doddema, H.J., Harder, W., 1993. Growth of the black yeast *Exophiala jeanselmei* on styrene and styrene-related compounds. Appl. Microbiol. Biotechnol. 39, 372–376.
De la Rosa, J.M., Martin-Sanchez, P.M., Sanchez-Cortes, S., Hermosin, B., Knicker, H., Saiz-Jimenez, C., 2017. Structure of melanins from the fungi *Ochroconis lascauxensis* and *Ochroconis anomala* contaminating rock art in the Lascaux Cave. Sci. Rep. 7, 13441.
Di Russo, C., Carchini, G., Rampini, M., Lucarelli, M., Sbordoni, V., 1997. Long term stability of a terrestrial cave community. Int. J. Speleol. 26, 7.
Diaz-Herraiz, M., Jurado, V., Cuezva, S., Laiz, L., Pallecchi, P., Tiano, P., Sanchez-Moral, S., Saiz-Jimenez, C., 2014. Deterioration of an Etruscan tomb by bacteria from the order Rhizobiales. Sci. Rep. 4, 3610.
Dollive, S., Peterfreund, G.L., Sherrill-Mix, S., Bittinger, K., Sinha, R., Hoffmann, C., Nabel, C.S., Hill, D.A., Artis, D., Bachman, M.A., Custers-Allen, R., Grunberg, S.,

Wu, G.D., Lewis, J.D., Bushman, F.D., 2012. A tool kit for quantifying eukaryotic rRNA gene sequences from human microbiome samples. Genome Biol. 13, R60.
Engel, A.S., Northup, D.E., 2008. Caves and karst as model systems for advancing the microbial sciences. In: Frontiers of Karst Research, Special Publication 13. Karst Water Institute, Lewisburg, PA, pp. 37–48.
Escudié, F., Auer, L., Bernard, M., Mariadassou, M., Cauquil, L., Vidal, K., Maman, S., Hernandez-Raquet, G., Combes, S., Pascal, G., 2018. FROGS: find, rapidly, OTUs with galaxy solution. Bioinformatics 34, 1287–1294.
Hammer, Ø., Harper, D., Ryan, P., 2001. PAST: paleontological statistics software package for education and data analysis. Palaeontol. Electron. 4, 1–9.
Harper, D.A.T., 1999. Numerical palaeobiology. Computer-based modelling and analysis of fossils and their distributions. Geol. Mag. 137, 463–479.
He, D., Wu, F., Ma, W., Gu, J.D., Xu, R., Hu, J., et al., 2022. Assessment of cleaning techniques and its effectiveness for controlling biodeterioration fungi on wall paintings of Maijishan Grottoes. Int. Biodeterior. Biodegrad. 171, 105406.
Herfort, L., Kim, J.-H., Coolen, M.J.L., Abbas, B., Schouten, S., Herndl, G.J., Damsté, J.S. S., 2009. Diversity of Archaea and detection of crenarchaeotal *amoA* genes in the rivers Rhine and Têt. Aquat. Microb. Ecol. 55, 189–201.
Herlemann, D.P., Labrenz, M., Jürgens, K., Bertilsson, S., Waniek, J.J., Andersson, A.F., 2011. Transitions in bacterial communities along the 2000 km salinity gradient of the Baltic Sea. ISME J. 5, 1571–1579.
Isola, D., Zucconi, L., Cecchini, A., Caneva, G., 2021. Dark-pigmented biodeteriogenic fungi in etruscan hypogeal tombs: new data on their culture-dependent diversity, favouring conditions, and resistance to biocidal treatments. Fungal Biol. 125, 609–620.
Jurado, V., Porca, E., Cuezva, S., Fernandez-Cortes, A., Sanchez-Moral, S., Saiz-Jimenez, C., 2010. Fungal outbreak in a show cave. Sci. Total Environ. 408, 3632–3638.
Jurburg, S.D., Nunes, I., Stegen, J.C., Le Roux, X., Priemé, A., Sørensen, S.J., Salles, J.F., 2017. Autogenic succession and deterministic recovery following disturbance in soil bacterial communities. Sci. Rep. 7, 45691.
Kiyuna, T., An, K.-D., Kigawa, R., Sano, C., Sugiyama, J., 2017. Noteworthy anamorphic fungi, *Cephalotrichum verrucisporum, Sagenomella striatispora,* and *Sagenomella griseoviridis*, isolated from biodeteriorated samples in the Takamatsuzuka and Kitora Tumuli, Nara, Japan. Mycoscience 58, 320–327.
Lharti, H., 2023. Caractérisation et modélisation thermo-physique des matériaux dans un milieu hétérogène. Application à la grotte de Lascaux. Doctoral dissertation,. Université de Bordeaux.
Magoč, T., Salzberg, S.L., 2011. FLASH: fast length adjustment of short reads to improve genome assemblies. Bioinformatics 27, 2957–2963.
Mahé, F., Rognes, T., Quince, C., de Vargas, C., Dunthorn, M., 2014. Swarm: robust and fast clustering method for amplicon-based studies. PeerJ 2, e593.
Martin-Sanchez, P.M., Miller, A.Z., Saiz-Jimenez, C., 2015. Lascaux Cave: an example of fragile ecological balance in subterranean environments. In: Microbial Life of Cave Systems. De Gruyter, pp. 279–302.
Martin-Sanchez, P.M., Nováková, A., Bastian, F., Alabouvette, C., Saiz-Jimenez, C., 2012. Use of biocides for the control of fungal outbreaks in subterranean environments: the case of the Lascaux Cave in France. Environ. Sci. Technol. 46, 3762–3770.
Miller, A.Z., García-Sánchez, A.M., L. Coutinho, M., Costa Pereira, M.F., Gázquez, F., Calaforra, J.M., Forti, P., Martínez-Frías, J., Toulkeridis, T., Caldeira, A.T., Saiz-Jimenez, C., 2020. Colored microbial coatings in show caves from the Galapagos Islands (Ecuador): first microbiological approach. Coatings 10, 1134.
Northup, D.E., 1997. Balancing Conservation of Unusual Cave Microbial Communities with Exploration and Research in Lechuguilla Cave, Carlsbad Caverns National Park, New Mexico. Final report to the Lindburgh foundation and the national park service.
Odum, E.P., 1969. The strategy of ecosystem development. Science 164, 262–270.
Ogórek, R., Višňovská, Z., Tančinová, D., 2016. Mycobiota of underground habitats: case study of harmanecká cave in Slovakia. Microb. Ecol. 71, 87–99.
Pfendler, S., Karimi, B., Maron, P.-A., Ciadamidaro, L., Valot, B., Bousta, F., Alaoui-Sosse, L., Alaoui-Sosse, B., Aleya, L., 2018. Biofilm biodiversity in French and Swiss show caves using the metabarcoding approach: first data. Sci. Total Environ. 615, 1207–1217.
Portillo, M.C., Gonzalez, J.M., Saiz-Jimenez, C., 2008. Metabolically active microbial communities of yellow and grey colonizations on the walls of Altamira Cave, Spain. J. Appl. Microbiol. 104, 681–691.
Quast, C., Pruesse, E., Yilmaz, P., Gerken, J., Schweer, T., Yarza, P., Peplies, J., Glöckner, F.O., 2013. The SILVA ribosomal RNA gene database project: improved data processing and web-based tools. Nucleic Acids Res. 41, D590–D596.
R Core Team, 2020. R: A Language and Environment for Statistical Computing. R Foundation for Statistical Computing, Vienna, Austria. http://www.R-project.org/.
Rognes, T., Flouri, T., Nichols, B., Quince, C., Mahé, F., 2016. VSEARCH: a versatile open-source tool for metagenomics. PeerJ 4, e2584.
Sakr, A.A., Ghaly, M.F., Edwards, H.G.M., Ali, M.F., Abdel-Haliem, M.E.F., 2020. Involvement of *Streptomyces* in the deterioration of cultural heritage materials through biomineralization and bio-pigment production pathways: a review. Geomicrobiol. J. 37, 653–662.
Shannon, C.E., 1948. A mathematical theory of communication. Bell Syst. Tech. J. 27, 623–656.
Simpson, E.H., 1949. Measurement of diversity. Nature 163, 688–688.
Spilde, M.N., Northup, D.E., Boston, P.J., Schelble, R.T., Dano, K.E., Crossey, L.J., Dahm, C.N., 2005. Geomicrobiology of cave ferromanganese deposits: a field and laboratory investigation. Geomicrobiol. J. 22, 99–116.
Steelman, K.L., Lombera-Hermida, A. de, Viñas-Vallverdú, R., Rodríguez-Álvarez, X.P., Carrera-Ramírez, F., Rubio-Mora, A., Fábregas-Valcarce, R., 2017. Cova Eirós: an integrated approach to dating the earliest known cave art in NW Iberia. Radiocarbon 59, 151–164.
Uroz, S., Calvaruso, C., Turpault, M.-P., Frey-Klett, P., 2009. Mineral weathering by bacteria: ecology, actors and mechanisms. Trends Microbiol. 17, 378–387.
Uroz, S., Kelly, L.C., Turpault, M.-P., Lepleux, C., Frey-Klett, P., 2015. The mineralosphere concept: mineralogical control of the distribution and function of mineral-associated bacterial communities. Trends Microbiol. 23, 751–762.
Yin, Q., Sun, Y., Li, B., Feng, Z., Wu, G., 2022. The r/K selection theory and its application in biological wastewater treatment processes. Sci. Total Environ. 824, 153836.
Zhang, J., Madden, T.L., 1997. PowerBLAST: a new network BLAST application for interactive or automated sequence analysis and annotation. Genome Res. 7, 649–656.
Zhao, J., Zeng, J., de Hoog, G.S., Attili-Angelis, D., Prenafeta-Boldú, F.X., 2010. Isolation and identification of black yeasts by enrichment on atmospheres of monoaromatic hydrocarbons. Microb. Ecol. 60, 149–156.
Zhou, J., Ning, D., 2017. Stochastic community assembly: does it matter in microbial ecology? Microbiol. Mol. Biol. Rev. 81, e00002, 17.
Zucconi, L., Gagliardi, M., Isola, D., Onofri, S., Andaloro, M.C., Pelosi, C., Pogliani, P., Selbmann, L., 2012. Biodeterioration agents dwelling in or on the wall paintings of the Holy Saviour's cave (Vallerano, Italy). Int. Biodeterior. Biodegrad. 70, 40–46.